BRCA1 Interactors - Rad50 and BRIP1: As Prognostic and Predictive Molecules for the Severity of Triple-Negative Breast Cancer

Suparna Laha (lahasuparna@gmail.com)
Yenepoya University
Muhseena N Katheeja
Yenepoya University
Shankar Das
Yenepoya University
Ranajit Das
Yenepoya University

Research Article

Keywords: DNA damage, overall survival, Tumour suppressor, Homologous recombination, Non-homologous end-joining repair, luminal A, Breast cancer, BRCA1

Posted Date: December 2nd, 2021

DOI: https://doi.org/10.21203/rs.3.rs-1084603/v1

Abstract

BRIP1 is one of the major interacting partner of *BRCA1* which plays an important role in repair by homologous recombination (HR). This gene is mutated in around 4% cases of breast cancer, however, its mechanism of action is unclear. In this study, we presented the fundamental role of BRCA1 interactors BRIP1 and RAD50 in the development of differential severity in Triple-Negative Breast Cancer(TNBC) among various affected individuals. We showed that in some TNBC lines like MDA-MB-231 the functioning of both BRCA1/TP53 is compromised. Furthermore, the sensing of DNA damage is affected, depicted through the low expression of damage sensing molecule Rad50 and reduced formation of H2AX foci. Due to less damage sensing capability and low availability of BRCA1 at the damage sites, the repair by HR becomes inefficient leading to more damage. Accumulation of damage sends a signal for over activation of NHEJ repair pathways. Over expressed NHEJ molecules with compromised HR and checkpoint conditions lead to higher proliferation and error-prone repair, which increases the mutation rate and corresponding tumor severity. The severity phenotypes were more in cells having compromised BRCA1-BRIP1 functioning. The *in silico* analysis of the TCGA-UCSC xena datasets with genes expression in deceased population shows a significant correlation of BRCA1 expression with OS in TNBCs (0.0272). The association of BRCA1 with OS becomes stronger with the addition of BRIP1expression (0.000876**). Since the overall survival(OS) is directly proportional to the extent of severity, the data analysis hints at the role of BRIP1 in controlling the severity of TNBC.

Introduction

Breast Cancer (BC) is the second leading cause of cancer related death in women (11.7% of all cases) and was identified to be a heterogeneous disease at the molecular level [1]. Estrogen receptor (ER), progesterone receptor (PR) and HER2 markers are used for prognostic identification of BC followed by appropriate targeted therapies [2]. For a better understanding of the heterogeneity of breast cancer; it is classified into 6 intrinsic subtypes, namely, luminal A, luminal B, HER2-enriched, claudin-low, basal-like and a normal breast-like group [3]. TNBC is characterised by its absence of the target receptors like ER, PR and HER2. An estimate of 1,70,000 cases (10-20%) of those diagnosed with breast cancer was categorized as TNBC[4]. Due to lack of receptors, it shows a poor prognosis followed by aggressive behaviour which leads to increased metastasis and decreased survival rate [5]. Specific target molecules and their interactors and mechanism of action at the molecular level remains unclear in TNBC. The genes involved in breast cancer, causing moderate risk are *BRIP1, CHEK2*, *ATM*, *RAD51C* and *PALB2* [6]. Several studies have investigated the role played by TP53 and BRCA1 gene. TP53 has a role in activating the cell cycle checkpoints. Breast cancers with *BRCA1* mutation carriers are frequently categorized as triple-negative basal-like and the prevalence rate is around 80-90% [7]. TP53 mutation is found in 20-35% of breast tumours and the mutation rate increase in TNBC to >90% [8, 9]. Recent clinical studies suggest that *BRCA1*$^{+}$*TP53*$^{+}$ TNBC cases had better overall survival chances than *BRCA1*$^{-}$*TP53*$^{-}$ cases and infact the survival ability of the breast cancer patients goes down when both *BRCA1* and *TP53* are affected [10]. The aggressiveness in the disease manifestation within the TNBC group shows individual variation and

the lack of receptors is unlikely to be the reason for this. Rather it is a condition that develops due to the interplay of several genes [11]. The current studies aim at addressing the molecular association of BRCA1 and TP53 with the severity of breast cancer manifestation.

BRIP1 is a helicase that interacts with BRCA1, through the BRCT domain and contributes to the DNA damage repair function of BRCA1 through homologous recombination [12]. Mutation at the interacting domains lead to the loss of BRCA1-BRIP1 interaction and consequently, less repair molecules reach the damaged sites. So the interaction of BRCA1 with BRIP1 ensures the suppression of the mutation prone non -homologous end joining mechanism of repair and promote double-strand DNA repair via the activation of HR [13]. The repair process also depends on the several damage sensing molecules. MRN complex consisting of RAD50, MRE11, and NBS1 plays a major role in DNA damage detection and maintaining active ATMs at the site of double-strand DNA break [14, 15]. The active ATMs or PI3-K like kinases phosphorylates H2AX at serine-139. The phosphorylated H2AX is required for DNA damage signal amplification and subsequent accumulation of numerous DDR proteins like BRIP1 at DSBs to form damage-induced foci. Once the γ-H2AX forms the foci, other DNA damage response proteins come and bind to the site of damage, accumulate and activate the repair activity [16]. H2AX and the associated proteins which are there in the damage induced foci also help to accumulate and promote to hold the broken ends together, thereby allowing time for DNA repair and minimizing the risk of misrepair [17].

In this paper, we present an *in-vitro* study with TNBC and Luminal BC along with experimental control samples focusing on the expression and specific functional roles played by the major breast cancer related oncogenes *BRCA1* and *TP53* and their interactor genes *BRIP1* and *RAD50*. We also performed an *in silico* analysis on the expressional level of the same genes in tissues at different disease conditions like TNBC, Luminal type, and compared them with solid normal tissue from the TCGA database and analysed their correlation and roles played in prognosis of the disease. We observed a differential expression pattern of TP53 and BRCA1 and the integrity of nuclear arrangement varies within different TNBC lines. The DNA damage sensing and response mechanisms through BRIP1 also change with different TNBC lines. In certain TNBC conditions, due to inefficient repair and in absence of checkpoints, stemness behaviour, metastatic property and high proliferation rate develops making the tumor more aggressive and severe. The combined expression pattern of BRCA1, BRIP1, and TP53 is highly associated with the diceased population of TNBC patients (*P* value 0.0055^{**}) compared to luminal type and control. In conclusion, the overall survivability is deeply affected when overexpression of BRIP1 comes in combination with $BRCA1^{+}$ and $TP53^{+}$.

Results

Differential expression of TP53 and BRCA1 within triple negative breast cancer group.

Clinical data suggest that TNBC cases with both BRCA1 and TP53 expression had better overall survival compared to cases that don't have their expression [10]. When we analyzed the expression of the transcripts of BRCA1 and TP53 in different breast cancer groups, in the patient data taken from the TCGA

database, we observed a significantly compromised expression of both the transcripts in the TNBC group. (Supp. Fig.1). But, clinical findings suggest a differential prognosis of TNBC from patient to patient. So there may be a differential expression of both the genes within triple-negative breast cancer conditions. To confirm this we performed the expression studies of these genes in different TNBC lines like MDA-MB-231 and MDA-MB-468. Another breast cancer subtype MCF7, as an experimental control and a normal cell line like HEK293T, were included in the experiments. We observed the difference in transcript levels of BRCA1 and TP53, in different lines of TNBC as anticipated. The mRNA expression of both TP53 and BRCA1 were significantly compromised in MDA-MB-231, one TNBC condition, compared to the non-cancerous cell line (HEK293T). The expression of both the genes was also significantly compromised in MDA-MB-231 compared to MDA-MB-468 (Fig. 1A, B). But, when we compared the average transcript levels of TP53 and BRCA1 in TNBC cell lines as a group with a different subgroup of breast cancer like the luminal type we observed the same compromised expression of both the transcripts as coming up in patient data analysis (Fig. 1C). Further analysis of the expressions of TP53 and BRCA1 in the different cell lines revealed that there is no correlation between TP53 and BRCA1 in case of ER/PR+ve condition and MDA-MB-468, just like wild type. Rather, we observed a moderate negative correlation between TP53 and BRCA1 protein in the MDA-MB-468 TNBC cell line (r = - 0.06501). But in the case of MDA-MB-231, BRCA1 seems to correlate with TP53 significantly with both having less expression (r=0.587). A similar correlation between the two genes was reflected in the *in silico* mRNA data analysis of the data collected from the TCGA database. Depending on correlation, TNBC is divided into two subgroups and MDA-MB-231 fall in the TNBC severe group (Fig. 1D). The experimental observations with MDA-MB-231 falls in line with the *in silico* mRNA data analysis of the severe TNBC cases where a correlation between TP53 and BRCA1 develops (r = 0.274, Fig.1D).

To further understand the effect of differential expression of BRCA1 and TP53 we studied the functioning of these transcripts in different TNBC cell lines. To understand the functional activity of TP53, we performed western blot analysis both for TP53 as well as phosho TP53. Whenever the DNA is challenged or integrity is compromised the major checkpoint kinase TP53 gets phosphorylated to activate the downstream mechanisms of cell cycle arrest and repair [9]. We observed TP53 is significantly overexpressed (P = 0.0293) in MDA-MB-468 compared to MDA-MB-231. We also found compromised phosphorylation of TP53 in MDA-MB-231 compared to MDA-MB-468, P = 0.0424(Fig. 1E, F). To understand the functional activity of BRCA1, we analysed the formation of BRCA1 foci at the damage sites, if at all there is any damage. BRCA1 is involved in the recognition and repair of aberrant structures in DNA and so with an increase in damage, BRCA1 foci are formed[18]. We observed the formation of BRCA1 foci to be significantly low in MDA-MB-231 compared to MDA-MB-468(P = 0.0041) (Fig.1G, H). So, our results likely indicate the robustness of checkpoint and repair proteins are compromised in one TNBC condition compared to the other and point towards differences in aggressiveness.

The integrity of the DNA changes with different TNBC lines:

As in the previous section, we showed a compromise in the activity of the checkpoint pathway as well as proper BRCA1 foci formation in MDA-MB-231, we were interested to observe the integrity of the DNA and

how significantly it varies within different TNBC lines. A perturbation in the genetic integrity shows a cell cycle arrest phenotype, so the cell cycle analysis was performed by staining the DNA content with PI (Fig.2A, B). We observed MDA-MB-231 cells to be mostly in G0/G1 and had a significantly low population of cells in the G2/M phase compared to MDA-MB-468 (P= 0.0095) as well as other cell types, inferring that it doesn't take much time at G2/M to maintain the genetic integrity, and completes the cell cycle very fast because of compromised checkpoint and repair (through BRCA1) functions. On contrary, the TNBC cell line MDA-MB-468 shows the same cell cycle profile as luminal type, MCF7 as well as the control line HEK293T which proves the proper functioning of the checkpoint and repair activity in MDA-MB-468 (Table 1). Further, we checked for the integrity of the DNA by staining the cells with DAPI. We had observed the compact homogeneous arrangement of the nucleus in the case of MDA-MB-468 and MCF7 but, MDA-MB-231 nuclei were not compact and the arrangement of the genetic material was found to be heterogeneous in nearly 54% of the cells as shown in Fig.2 C.D compared to only 27 % in MDA-MB-468 cells when analysed in 200 cells. To further confirm the damage in DNA we have performed the comet assay and observed the formation of tails (Fig. 2E). MDA-MB-231 cells showed high DNA damage with 9.7% of cells containing tails of fragmented DNA compared to MDA-MB-468 with 6% cells having fragmented DNA tail (P = 0.0035) (Fig. 2F). In the case of wild type cells, only 3% of the cells developed tails in the comet assay. The damage in the genetic material was also confirmed by performing Agarose gel electrophoresis at 50 Volts for 22 hours with the DNA extracted from these cell lines. We observed that MDA-MB-231 DNA moved fastest with a distance of 29.9 mm from the start point compared to the other TNBC line, MDA-MB-468, which was slower and traversed 25.4 mm only at the same time. MCF7 DNA moved almost the same as MDA-MB-468 with a distance of 24.4 mm from the start point. The DNA from the HEK293T cells could move only 23.3 mm because of its compact and bulky nature (Fig. 2G). So, the increase in a smear in the MDA-MB-231 lane confirms the increase in the fragmentation and fast movement of the DNA compared to MDA-MB-468 DNA with a lighter smaer.

DNA damage sensing abilities changes with different TNBC lines:

We showed that the integrity of genetic material differs between different TNBC lines. The increase of DNA fragmentation in MDA-MB-231 cells leads to the accumulation of more DNA damage, but surprisingly we saw compromised BRCA1 foci in MDA-MB-231 cells which develops at the damage sites. We, therefore, suspect an abrogation in DNA damage sensing capacity across the cell lines. So, we investigated the DNA damage sensing capacity in different BC lines and also in between the TNBCs by studying the DNA damage sensing molecules Rad50 and H2AX. Though we showed more DNA damage in MDA-MB-231, the expression of damage sensing molecule RAD50 didn't increase to the extent of DNA damage, rather RAD50, both in the transcript as well as protein level was down-regulated in MDA-MB-231 cells compared to MDA-MB-468 (Fig.3A,B,C). As RAD50 is low in MDA-MB-231 we further wanted to investigate the damage sensing defect by observing the gamma-H2AX foci. H2AX binds to breaks and nicks of DNA molecule produced during any insult on DNA and forms fewer bigger intense damage foci [19]. More number of smaller foci are also formed during the mitotic phase [20]. We have counted the H2AX foci in approximately 200 cells in each of the different cell types (Fig.3D). We have also analysed the colocalization of the BRCA1-H2AX foci to confirm the specificity of BRCA1 foci to the sensors and

justify the less number of BRCA1 dots in MDA-MB-231. We observed that BRCA1 protein is associated with almost 98% of the H2AX protein in all the cell types but observed more number of cells having no foci in MDA-MB-231. In the case of control cells HEK293T, cells with no foci are maximum as expected (Fig. 3E). Furthemore, in TNBC lines like MDA-MB-231, more intense BRCA1-H2AX foci with significantly less in number were formed compared to the other TNBC condition MDA-MB-468 cells (P-value 0.0001). The foci formation in MCF7 and HEK293T were also significantly high compared to MDA-MB-231 cells (P-value 0.0003) (Fig 3D, F). This proves that due to compromised DNA damage sensing molecule and shorter mitotic phase, the number of H2AX foci, as well as BRCA1 foci, are significantly less formed in MDA-MB-231(fig.3D, F). The absence of sensing the damage affects the downstream repair processes which lead to the accumulation of more DNA damage compared to other TNBC subtypes and luminal subtypes (MCF7). In conclusion due to compromised sensing of DNA damage, the repair of the damage sites is also compromised leading to accumulation of damage.

Upregulation of the repair pathway due to accumulated damage:

In our previous sections, we showed that in some cases of TNBC like MDA-MB-231, there is a complete compromised condition of the checkpoint, sensing of damage as well as BRCA1 functioning, leading to accumulated damage whereas the pathways are relatively well managed in another TNBC line MDA-MB-468. Accumulated damage will lead to upregulated repair pathways. So we further looked into the variations of the repair pathways in the two TNBC conditions. We checked the status of the repair molecules BRIP1 which repairs through homologous recombination and Ku70 which follows the Non-homologous end-joining pathway. We observed that BRIP1 is expressed more (Fig. 4A,B,C) in MDA-MB-231 cells when compared to MDA-MB-468 cells but the function is compromised as it doesn't reach the damage sites (less BRCA1 damage foci, Fig. 1G, 3D). We also confirmed the over functioning of the NHEJ pathway by showing the expression of Ku70 in MDA-MB-231 cells significantly high (fig4. A,B,D). The overexpression of Ku70 and BRIP1in MDA-MB-231 cells confirms the robustness of DNA repair. A robust NHEJ repair in presence of a compromised checkpoint as shown in the previous section happens in some TNBC conditions like MDA-MB-231 which increases the chances of an error-prone repair activity followed by accumulated mutation. More mutations add up to the complexity of tumorogenesis. To further correlate the role of these 3 genes, BRCA1, TP53 and BRIP1 in developing severe conditions we performed the *in silico* correlation analysis of BRCA1 interacting repair molecule, BRIP1 with checkpoints, in BC and TNBC patient group collected from the TCGA database. In fig.4E we found that though BRCA1 and BRIP1 correlates in all conditions, (normal, P = <0.0001, r = 0.703; ER/PR+ve, P= <0.0001 r = 0.473 and TNBC, P = 0.049, r = 0.19) there is no correlation between BRCA1 and TP53 in all the 3 conditions (normal, P = 0.897, r = -0.012; ER/PR+ve, P= 0.3252 r = -0.056 and TNBC, P = 0.212, r = -0.121). Whereas in case of severe TNBC condition, all the 3 proteins are significantly correlated (BRCA1/BRIP1: P = 0.008, r = 0.813, BRCA1/TP53: P = 0.475, r = 0.274).

Severity is highly dependent on upregulated repair and compromised checkpoint pathways :

So far we showed the development of different conditions in different TNBC cell lines. Correlation analysis between BRCA1, BRIP1 and TP53 justifies the development of a condition where there is upregulated repair in absence of robust checkpoint and sensing of damage. This condition is prone to mutations[21]. Accumulated mutations will add up to the complexity of tumorogenesis. In this final section, we identified that the conditions developed in MDA-MB-231 develops severity compared to the mild conditions in MDA-MB-468. One of the hallmarks for severity is proliferation. In fig.5 A, B we have shown through immunophenotyping that more than 70% of the cells contain the proliferation marker, Ki67 in the case of the MDA-MB-231 cell compared to only 40-50% of cells approximately in MDA-MB-468 and MCF7(Fig.5A, B). We also looked at the expression of the transcription factor, BTB and CNC homology 1, BACH1, which has a role in metastasis, angiogenesis, and developing aggressive behaviour of tumor cells [22]. The expression of BACH1 protein was significantly more in MDA-MB-231 cells compared to HEK293T cells (P= 0.0078, Fig.5C ,D). We further analyzed the transcript level of BACH1 in all the cell lines and confirmed that the expression of BACH1 is significantly more in MDA-MB-231 compared to the rest of the lines (P = 0.0295, fig.5E). We also looked for the stemness property of the different TNBC cells as well as in different BC groups and control line by quantifying the cancer stem cell population through immunophenotyping. Fig.5F, G shows that there is a higher population of $CD44^+/CD24^-$ cells in MDA-MB-231 compared to MDA-MB-468 and other breast cancer line MCF7. The $CD44^+/CD24^-$ population was very less in the control line HEK293T (Fig5F, G). So in this section, we proved that MDA-MB-231 cells show stemness and metastatic properties. For further supporting that the condition developed by correlation of BRCA1/BRIP1/TP53 in MDA-MB-231 to be severe, we analysed the overall survival in TCGA patient data with the concerning proteins. The data shows that the expression of individual transcript (BRCA1 or BRIP1 or TP53) does not correlate with OS in the case of ER/PR+ve but in the case of TNBC, OS is associated with the overexpressed BRCA1(P = 0.0272, R^2 = 0.5254) (Table 2). Surprisingly, when expression of BRIP1 is considered along with BRCA1 and analysed for OS, only TNBCs have a significant increase in association with BRCA1/BRIP1 expression and OS (P = 0.0008706, R^2 = 0.9045) and finally when expression of all the 3 BRCA1, BRIP1 and TP53 is considered for their correlation with OS, a synergistic association with OS was observed over BRCA1/BRIP1 in TNBC patient only (P = 0.0055, R^2= 0.9048) (Table 2)

Discussion

TNBC shows aggressive behaviour, having a high rate of metastasis as well as an increased reoccurrence rate. Also, its prognosis is poor due to the lack of effective therapy [6]. In addition to all the complexities of this disease, its characters vary from one patient to another patient which has baffled clinicians. In this study, we addressed the likely reason behind the differential characteristics of TNBC cases. We studied the molecules and the mechanisms involved in TNBC progression/reoccurrence/metastasis and revealed the molecular factors that play a role in determining the severity of the disease. When different TNBC lines were considered as a group, we observed a similar loss of expression of TP53 and BRCA1, like ER/PR+ve breast cancer, compared to the normal epithelial cells. The experimental data is supported by the analysis of the patient data collected from publicly available datasets. But the expression profile of

the same genes in different TNBC cell lines doesn't follow the analysis performed on publicly available data. From our in vitro experiments, we observed that in some TNBC lines like MDA-MB- 231, the reduction in the expression of BRCA1 and TP53 is more compared with other triple-negative as well as ER/PR+ve breast cancer. But, in some, like MDA-MB-468, the expression of BRCA1/TP53 is discernibly higher than the ER/PR+ve condition. The formation of BRCA1 foci and phosphorylated TP53 was less in MDA-MB-231 insinuating the compromised functioning of the genes. The reduced functioning of the TP53 checkpoint allows the cells to move fast in the G2-phase taking less time to rectify the damage affecting the integrity of the DNA more in MDA-MB-231 cells as evident from less compact DNA and tails in the comet assay. But surprisingly the sensing of damage by RAD50 followed by the formation of γ-H2AX foci was significantly compromised in MDA-MB-231 cells. Less phosphorylated H2AX results in an unstable DDR complex at the damaged sites which in turn leads to impaired error-free HR activity through the BRCA1-BRIP1 axis [23, 24]. Whereas, in the case of MDA-MB-468, the MRN complex is more active, as evident from increased Rad50 expression. As a result, the number of H2AX followed by BRCA1 foci was more compared to the other TNBC line MDA-MB-231 and prefer repair of damaged DNA by HR. So, in some cases of TNBC, the damage is more due to compromised BRCA1 and the processing of the damage is also improper because of the absence of the other interacting proteins of BRCA1 like Rad50.

Abrogation in repair leads to the accumulation of more damage and expression of more repair molecules respectively as observed with the overexpression of the BRIP1 and Ku70 in MDA-MB-231. Overexpression of two arms of the DNA repair pathway simultaneously in TNBC cell lines, independent of BRCA mutation status, resulted in unrepairable DNA damage and subsequent cell death [25, 26]. As BRIP1 is unable to reach the functional site due to the absence of Rad50 followed by γ-H2AX, so to promote repair to the accumulated damage, the cells follow the NHEJ repair pathway resulting in DNA repair with accumulated mutations [27]. So, the chances of getting NHEJ repair are less when the functioning of BRCA1 is not compromised. An increase in mutations leads to more aggressive tumors [28]. The markers of aggressive tumorigenesis were observed more, in the case of MDA-MB-231 cells with higher Ki67 expression [29]. Ma *et.al*. has shown that CD44+ /CD24− cell population with cancer stem cell-like properties may play an important role in the aggressive behaviours of TNBC [30]. We also confirmed the increase in the stemness property of MDA-MB-231 cells, as more than 70% of the population of cells contain the cancer stem cell marker compared to the other TNBC (40%) and BC (6%) cell types(Fig. 5F,G). We observed the up-regulated expression of BACH1 in MDA-MB-231 cells too. BACH1 is a transcription factor having a role in tumor relapse and metastasis. So, from the above experiment, we conclude that MDA-MB-231 has the worst prognosis with higher chances of severity, aggressiveness, and metastasis than the MDA-MB-468 and MCF7 cell lines, an observation that is also in line with clinical observations.

Analysis of overall survival with the publicly available patient data confirms the same correlation of BRCA1, TP53 and BRIP1 with severity. The data shows that there is a correlation between BRCA1 and BRIP1 in breast cancer patients(Table 2). The expression of BRCA1 and BRIP1 is associated in luminal type (P = 0.0001) as well as TNBC (P =0.0077), but the OS is related with BRCA1 with a correlation of R^2 = 0.525 only in the case of TNBC (P =0.0272) (Table.2). The correlation of OS with BRCA1 in TNBC

increases(R^2 =0.9045, P = 0.00087) when BRIP1 is considered along with BRCA1. So, the decrease in overall survivability or increase in severity depends on the function of both the gene BRCA1 and BRIPI and also the combination of 3 genes i.e, BRCA1, BRIP1, and TP53 (P = 0.0055) in certain TNBC conditions. This data highly supports our experimental data, where we have concluded in the above section that less functioning of BRIP1, due to compromised BRCA1 activity leads to the severity with overexpression of proliferative, stemness, angiogenic and metastatic markers supporting the aggressive nature of cancer progression.

Thus we have defined the signalling cascade for the development of severity in TNBC. We identified the direct association of the DNA repair pathway with the severity of breast cancer. This is supported by the fact that compromised checkpoint and less functional BRCA1 leads to more accumulated damage. Also, low sensing of damage through Rad50 and H2AX takes place leading to less BRCA1 at the damage sites. Less BRCA1 at damage sites leads to less HR through BRIP1. While the coexpression of BRCA1/TP53 supports the efficient repair activity through HR with less chance of recurrence/severity in MDA-MB-468, high expression of Ku70 leads to error-prone NHEJ repair activity in MDA-MB-231, developing the chance of mutations at the molecular level. More mutations lead to severe conditions in certain TNBC cases which can be visible by more tumorigenic phenotypes. Hence understanding of the breast cancer subtypes is essential in terms of personalized medicine and our study throws light on the aggressiveness of one of the subtypes of breast cancer which happens as a result of lack of efficient repair activity due to compromised sensing of DNA damage and promotion of error-prone repair activity.

Materials And Methods

Cell line and cell culture

Human TNBC cell lines MDA-MB-231 and MDA-MB-468, Luminal cell lines MCF7, and control Cell line HEK293T, purchased from the National Centre for Cell Science, Pune, India were cultured as given in the datasheet provided by the repository.

Total RNA isolation and qRT-PCR for mRNA detection

RNA from mammalian cells were isolated using triazole reagents according to manufacturer protocol (Sigma, Catalog number- T9424) [31]. Briefly, 500 ng of total RNA was converted to cDNA with the iScript cDNA synthesis kit (Thermo Fisher Scientific). RT–PCR was performed with diluted cDNA (1:50) using SYBR Green master mix (Dynamo color flash SYBR Green qPCR kit, #F4167l) and primer sequences of the genes of interest taking GAPDH as housekeeping gene (Table 3). All samples were processed in triplicate. $\Delta\Delta C_t$ value was calculated using the C_t values of the housekeeping gene and the NTCs.

Western blotting

To isolate protein from the cells Jang *et. al.* protocol was followed [32]. 50 ug of protein was loaded on 8 to 10 % -SDS PAGE depending on the size of the protein. The westerns were performed as given in Gouda

et al.[33]. The antibody details for all the proteins are listed in Supplementary Table 1.

Cell cycle analysis:

The cells (0.5M cells/ml) were processed for flow cytometry according to the protocol in reference [34]. Trypsinised cells were washed with 1X PBS and incubated with hypotonic DNA staining solution (0.5 mg/ml propidium iodide, 0.1% sodium citrate, and 0.05% Triton X-100) for 15 minutes at room temperature. The lysed cells were washed off from excess PI and analyzed by a Guava easycyte flow cytometer for the cell cycle. 5000 events were analyzed from each sample.

Immunophenotyping:

5×10^5 cells were incubated with 500 ul of FACS Staining buffer (FBS 2%, EDTA 0.5M stock pH 8, PBS and 1% Antibiotics) for 15 minutes and then washed with 1X PBS. The cell suspension was incubated with different conjugated /non-conjugated antibodies (Supp. Table 1) at the concentration recommended by the manufacturer for 45 min at 4°C in dark. The labelled cells were washed and resuspended with FACS staining buffer. Samples were analyzed using a guava easycyte flow cytometer.

DAPI Staining:

5×10^5 cells were seeded on collagen-coated coverslips in each well of a 6-well plate. At 80% confluency, cells were washed with PBS and fixed in 4% paraformaldehyde. Cells were stained and mounted with PD-DAPI solution (0.5 µg/ml DAPI in 90% glycerol containing 1mg/ml of the anti-fade dye *p*-phenylenediamine). The percentage of cells with heterogeneously stained DNA was carried out by quantitative analysis (counting ≥ 200 cells for each sample in n=3 experiments.).

Immunofluorescent assay (IFA):

5×10^4 cells were seeded on collagen-coated coverslips in each well of a 6-well plate. At 80% confluency, cells were washed with 1X PBS and fixed in 4% paraformaldehyde followed by permeabilization with 0.3% triton-X 100 in 1X PBS for 10 minutes each. Blocking was done for 1 hr with 5% FBS in 1X PBS at room temperature. The cells were incubated with primary antibodies overnight at 4°C in humid conditions followed by the corresponding secondary antibody for 1 hour at room temperature. 3 times washing with 1X PBS was given after each antibody treatment. Coverslip containing cells were mounted on the glass slide with 10 ul of PD-DAPI and imaging was done using an EVOS-M5000 microscope.

Comet assay:

Comet assay was performed as given in Olive et al.,2006 with slight modification [35]. Cell pellets containing 5000 cells were suspended in 0.8% low melting agarose in 0.9% saline solution, mixed well, and poured onto the frosted slide, the coverslip was placed over the gel. After solidification, it was incubated in freshly prepared lysis solution (2.5M NaCl, 100Mm Na. EDTA, 1% Triton-X 100, 10% DMSO) at 4°C overnight, washed with freshly prepared alkaline buffer (300Mm NaOH, 1Mm NaEDTA, PH.13)

followed by electrophoresis at 24V for 30 minutes. Slides were washed with 0.4M Tris-base and stained with EtBr solution. Imaging was done using Zoe fluorescent imager (Biorad).

DNA extraction and Agarose gel electrophoresis

DNA from the mammalian cells was extracted by using the phenol-chloroform method. Briefly, for the fresh cell pellet, 875 ul of TE buffer was added and mixed well for the same tube 100 ul of 10% SDS and 1ml of the phenol-chloroform mixture is added and incubated at room temperature for 5-10 minutes. After the centrifugation at 4^0C for 10 minutes, the upper viscous supernatant was collected to a fresh tube. DNA precipitation was done by mixing gently with 100ul of 5M sodium acetate. 2ml of Isopropanol was added and mixed by inversion until the white DNA strands get separated. The mixture was centrifuged and collected the DNA followed by 75% EtOH wash. The DNA pellet was dissolved in TE buffer. The quantification was done using nanodrop colibre. 1-2 ug of DNA was loaded in 0.7% agarose, ran for around 22 hrs. at 50 V and visualized under gel documentation system.

In silico data analysis

Gene expression data for TNBC, luminal type, and solid tissue normal data were downloaded from TCGA using UCSC Xena [36]. For phenotypes (N=1236) as well as gene expression RNA seq data (N=1218) was downloaded as log2 (x+1) transformed RSEM normalized count values. The expression of the different genes in TNBC (N=109), ER/PR^{+ve} (N=371), and solid normal tissue (N=119) were filtered. The association between gene expression of an individual gene and combinational genes was performed using R v3.6.3. Overall survival (OS) was analyzed only in the diceased population (N=9) concerning specific gene expression using Pearson's correlation test. Data can be provided on request.

Statistical analysis

All laboratory experiments were carried out minimum in biological triplicate and technical triplicates as and where required. Statistical analysis was performed using Graph Pad Prism (v8.0). The gene expression was compared by one-way/two-way analysis of variance followed by Tukey's multiple comparisons. Paired T-test and Pearson correlation test were also performed when required. Potential outliers were identified using the rout method (Q=10) implemented in Graph Pad Prism [37]. P-value <0.05 was considered statistically significant.

Declarations

Approval to the study:

The study is approved by Scientific Review Board (SRB no: YRC-SRB/022/2018) from Yenepoya research centre, Yenepoya (Deemed to be) University, Mangalore, Karnataka, India and supported by Seed Grant (YU/seedgrant/055-2016.05-08-2016) from Yenepoya (Deemed to be) University. Ethical clearance is not required for the study.

Availability of data

The data generated and analysed that support the current findings are available on request from the corresponding author [*Dr. Suparna Laha*]. The analysed data sets are publicly available [UCSC xena-TCGA] repository [doi: https://doi.org/10.1101/326470] [38].

Acknowledgements

I would like to acknowledge Yenepoya Deemed to be a University for providing the Seed grant project and the facility to carry out the research. I would like to acknowledge GOKDOM (Government of Karnataka Department of Minority) for providing the fellowship to K.M.N (CR-97/2018-19). I would like to acknowledge Mr. Amjad Hussain and Ms. Mithila Kulkarni for helping me in performing the experiments and Mr. Sooraj Mutthukada for helping me with data analysis.

Competing Interests

The authors declare that they have no competing financial interests.

References

1. Sung H, Ferlay J, Siegel RL, Laversanne M, Soerjomataram I, Jemal A, Bray F. Global cancer statistics 2020: GLOBOCAN estimates of incidence and mortality worldwide for 36 cancers in 185 countries. CA: A Cancer Journal for Clinicians. 2021 May;71(3):209-49.https://doi.org/10.3322/caac.21660
2. Dai X, Xiang L, Li T, Bai Z. Cancer hallmarks, biomarkers and breast cancer molecular subtypes. Journal of Cancer. 2016;7(10):1281. doi: 10.7150/jca.13141
3. Dai X, Li T, Bai Z, Yang Y, Liu X, Zhan J, Shi B. Breast cancer intrinsic subtype classification, clinical use and future trends. American journal of cancer research. 2015;5(10):2929.
4. Aysola K, Desai A, Welch C, Xu J, Qin Y, Reddy V, Matthews R, Owens C, Okoli J, Beech DJ, Piyathilake CJ. Triple negative breast cancer–an overview. Hereditary genetics: current research. 2013 Jan 1;2013(Suppl 2). doi: 10.4172/2161-1041.S2-001
5. Yadav BS, Chanana P, Jhamb S. Biomarkers in triple negative breast cancer: a review. World journal of clinical oncology. 2015 Dec 10;6(6):252. doi: 10.5306/wjco.v6.i6.252
6. Foretova L, Navratilova M, Svoboda M, VasickovaP, Stahlova EH, Házova J, Kleiblova P, Kleibl Z, Machackova E, Palacova M, Petrakova K. Recommendations for Preventive Care for Women with Rare Genetic Cause of Breast and Ovarian Cancer. Klinicka onkologie: casopis Ceske a Slovenske onkologicke spolecnosti. 2019 Jan 1;32(Supplementum2):6-13. DOI: 10.14735/amko2019S6
7. Godet I, Gilkes DM. BRCA1 and BRCA2 mutations and treatment strategies for breast cancer. Integrative cancer science and therapeutics. 2017 Feb;4(1). doi: 10.15761/ICST.1000228
8. Chae BJ, Bae JS, Lee A, Park WC, Seo YJ, Song BJ, Kim JS, Jung SS. p53 as a specific prognostic factor in triple-negative breast cancer. Japanese journal of clinical oncology. 2009 Apr 1;39(4):217-24. DOI: 10.1093/jjco/hyp007

9. Chen J. The cell-cycle arrest and apoptotic functions of p53 in tumor initiation and progression. Cold Spring Harbor perspectives in medicine. 2016 Mar 1;6(3):a026104. doi: 10.1101/cshperspect.a026104
10. Kim MC, Choi JE, Lee SJ, Bae YK. Coexistent loss of the expressions of BRCA1 and p53 predicts poor prognosis in triple-negative breast cancer. Annals of surgical oncology. 2016 Oct;23(11):3524-30. DOI: 10.1245/s10434-016-5307-z
11. Feng Y, Spezia M, Huang S, Yuan C, Zeng Z, Zhang L, Ji X, Liu W, Huang B, Luo W, Liu B. Breast cancer development and progression: Risk factors, cancer stem cells, signaling pathways, genomics, and molecular pathogenesis. Genes & diseases. 2018 Jun 1;5(2):77-106. https://doi.org/10.1016/j.gendis.2018.05.001.
12. Muhseena K N, Mathukkada S, Das SP, and Laha S. The repair gene *BACH1* - a potential oncogene. Oncol Rev. 2021 Feb 26; 15(1): 519. doi: 10.4081/oncol.2021.519
13. Cantor SB, Bell DW, Ganesan S, Kass EM, Drapkin R, Grossman S, Wahrer DC, Sgroi DC, Lane WS, Haber DA, Livingston DM. BACH1, a novel helicase-like protein, interacts directly with BRCA1 and contributes to its DNA repair function. Cell. 2001 Apr 6;105(1):149-60. https://doi.org/10.1016/S0092-8674(01)00304-X
14. Lavin MF. ATM and the Mre11 complex combine to recognize and signal DNA double-strand breaks. Oncogene. 2007 Dec;26(56):7749-58.
15. Syed A, Tainer JA. The MRE11–RAD50–NBS1 complex conducts the orchestration of damage signaling and outcomes to stress in DNA replication and repair. Annual review of biochemistry. 2018 Jun 20;87:263-94. https://doi.org/10.1146/annurev-biochem-062917-012415
16. Lowndes NF, Toh GW. DNA repair: the importance of phosphorylating histone H2AX. Current biology. 2005 Feb 8;15(3):R99-102. https://doi.org/10.1016/j.cub.2005.01.029
17. Yuan J, Adamski R, Chen J. Focus on histone variant H2AX: to be or not to be. FEBS letters. 2010 Sep 10;584(17):3717-24.https://doi.org/10.1016/j.febslet.2010.05.021
18. Wang Y, Cortez D, Yazdi P, Neff N, Elledge SJ, Qin J. BASC, a super complex of BRCA1-associated proteins involved in the recognition and repair of aberrant DNA structures. Genes & development. 2000 Apr 15;14(8):927-39.
19. Cannan WJ, Pederson DS. Mechanisms and Consequences of Double-Strand DNA Break Formation in Chromatin. J Cell Physiol., 2016 Jan;231(1):3-14. doi: 10.1002/jcp.25048.
20. Cabrero J, Teruel M, Carmona FD, Camacho JP. Histone H2AX phosphorylation is associated with most meiotic events in grasshopper. Cytogenetic and genome research. 2007;116(4):311-5. https://doi.org/10.1159/000100416
21. Chatterjee N, Walker GC. Mechanisms of DNA damage, repair, and mutagenesis. Environmental and molecular mutagenesis. 2017 Jun;58(5):235-63. doi: 10.1002/em.22087
22. Zhang X, Guo J, Wei X, Niu C, Jia M, Li Q, Meng D. Bach1: function, regulation, and involvement in disease. Oxidative medicine and cellular longevity. 2018 Oct 2;2018.

23. Zimmermann M, de Lange T. 53BP1: pro choice in DNA repair. Trends in cell biology. 2014 Feb 1;24(2):108-117.
24. Krum SA, Dalugdugan ED, Miranda-Carboni GA, Lane TF. BRCA1 forms a functional complex with-H2AX as a late response to genotoxic stress. Journal of nucleic acids.2010 Volume 2010, Sept. 27, 9 pages. https://doi.org/10.4061/2010/801594
25. Boerner JL, Nechiporchik N, Mueller KL, Polin L, Heilbrun L, Boerner SA, Zoratti GL, Stark K, LoRusso PM, Burger A. Protein expression of DNA damage repair proteins dictates response to topoisomerase and PARP inhibitors in triple-negative breast cancer. PLoS One. 2015 Mar 16;10(3):e0119614.DOI: 10.1371/journal.pone.0119614
26. Alshareeda AT, Negm OH, Albarakati N, Green AR, Nolan C, Sultana R, Madhusudan S, Tighe P, Ellis IO, Rakha EA. Clinicopathological significance of Ku70/Ku80, a key DNA damage repair protein in breast cancer. Breast cancer research and treatment. 2013 Jun;139(2):301-10.
27. Chiruvella KK, Liang Z, Wilson TE. Repair of double-strand breaks by end joining. Cold Spring Harbor perspectives in biology. 2013 May 1;5(5):a012757. doi: 10.1101/cshperspect.a012757
28. Takahashi H, Asaoka M, Yan L, Rashid OM, Oshi M, Ishikawa T, Nagahashi M, Takabe K. Biologically aggressive phenotype and anti-cancer immunity counterbalance in breast cancer with high mutation rate. Scientific reports. 2020 Feb 5;10(1):1-3.
29. Blagosklonny MV. Target for cancer therapy: proliferating cells or stem cells. Leukemia. 2006 Mar;20(3):385-91.
30. Ma F, Li H, Wang H, Shi X, Fan Y, Ding X, Lin C, Zhan Q, Qian H, Xu B. Enriched CD44+/CD24− population drives the aggressive phenotypes presented in triple-negative breast cancer (TNBC). Cancer letters. 2014 Oct 28;353(2):153-9. https://doi.org/10.1016/j.canlet.2014.06.022
31. Chomczynski P, Sacchi N. Single-step method of RNA isolation by acid guanidinium thiocyanate-phenol-chloroform extraction. Analytical biochemistry. 1987 Apr 1;162(1):156-9. https://doi.org/10.1016/0003-2697(87)90021-2
32. Jang HM, Lee KE, Kim DH. The preventive and curative effects of Lactobacillus reuteri NK33 and Bifidobacterium adolescentis NK98 on immobilization stress-induced anxiety/depression and colitis in mice. Nutrients. 2019 Apr;11(4):819. https://doi.org/10.3390/nu11040819
33. Gouda MM, Prabhu A, Bhandary YP. Curcumin alleviates IL17A mediated p53 PAI1 expression in bleomycin induced alveolar basal epithelial cells. Journal of cellular biochemistry. 2018 Feb;119(2):2222-30. DOI 10.1002/jcb.26384
34. Shen D, Wu G, Suk HI. Deep learning in medical image analysis. Annual review of biomedical engineering. 2017 Jun 21;19:221-48. https://doi.org/10.1146/annurev-bioeng-071516-044442
35. Olive PL, Banáth JP. The comet assay: a method to measure DNA damage in individual cells. Nature protocols. 2006 Jun;1(1):23.
36. Goldman M, Craft B, Brooks A, Zhu J, Haussler D. The UCSC Xena Platform for cancer genomics data visualization and interpretation. biorxiv. 2018 Jan 1:326470. doi: https://doi.org/10.1101/326470

37. Motulsky HJ, Brown RE. Detecting outliers when fitting data with nonlinear regression–a new method based on robust nonlinear regression and the false discovery rate. BMC bioinformatics. 2006 Dec;7(1):1-20.

Tables

Due to technical limitations, tables are only available as a download in the Supplemental Files section.

Figures

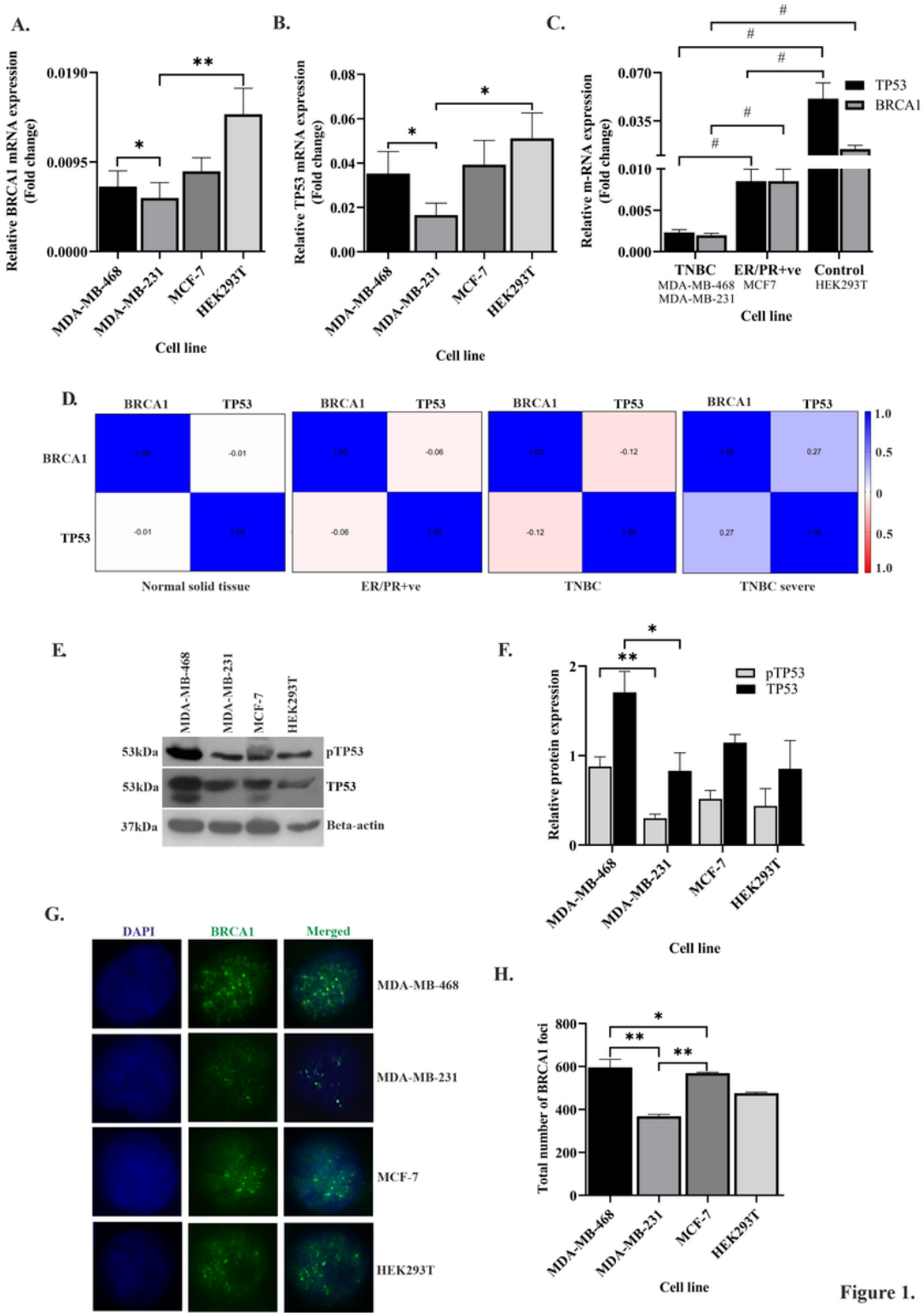

Figure 1.

Figure 1

Differential expression of TP53 and BRCA1 within TNBC cells. A and B. BRCA1 and TP53 expression changes with TNBC condition: The bar graph represents the expression studies done with c-DNA (500 ng of RNA) from the TNBC cell line MDA-MB-468 and MDA-MB-231, luminal type MCF-7 and control line HEK293T. The expression was quantified from the technical triplicates of the RT qPCR data. C. Overall mRNA expression of both BRCA1/TP53 is less in TNBC group: The mRNA expression of both

BRCA1/TP53 in different cell lines of TNBC is taken together and considered as the TNBC group. The expressions are compared with ER/PR+ve subtype cells and normal cells and represented in graph. D. Association of BRCA1 and TP53 shows up in TNBC severe condition only: Association between BRCA1 and TP53 in different BC tissues condition obtained from TCGA data are analysed by correlogram. Moving towards darker blue colour indicates an increase in positive correlation, whereas towards darker red indicates an increase in negative correlation. White colour indicates no correlation. E. TP53 and its functioning are compromised in some TNBC condition: TP53 expression as well as its phosphorylation was detected by western blot analysis of proteins extracted from the above mentioned cells, using corresponding (TP53 and phosphor-TP53) antibodies. ß-actin is given as the loading control. F.Quantification of TP53 and pTP53 expression in TNBC cells: The intensity of the TP53 and its phosphorylated bands from Western blots were quantified using Image J software. The values of band intensities were normalized with the corresponding ß-actin to normalize the protein loading. G. Functioning of BRCA1 is also compromised in MDA-MB-231 condition: Functioning of BRCA1 molecule is visualised by the formation of BRCA1 foci in all the different cell lines in Immuno-fluorescence assay. H. Quantification of BRCA1-foci in TNBC cells: BRCA1-foci formation is scored in each cell and plotted as a bar-graph. The X-axis represents the different cell-line and Y-axis represents the total number of BRCA1 foci formed in 200 cells. All the experiments are done in biological triplicates. Data were analysed by one-way ANOVA, Pearson correlation test and paired T-test. (SEM is shown as error bars. *P< 0.05, ** P < 0.005 and # P<0.0001)

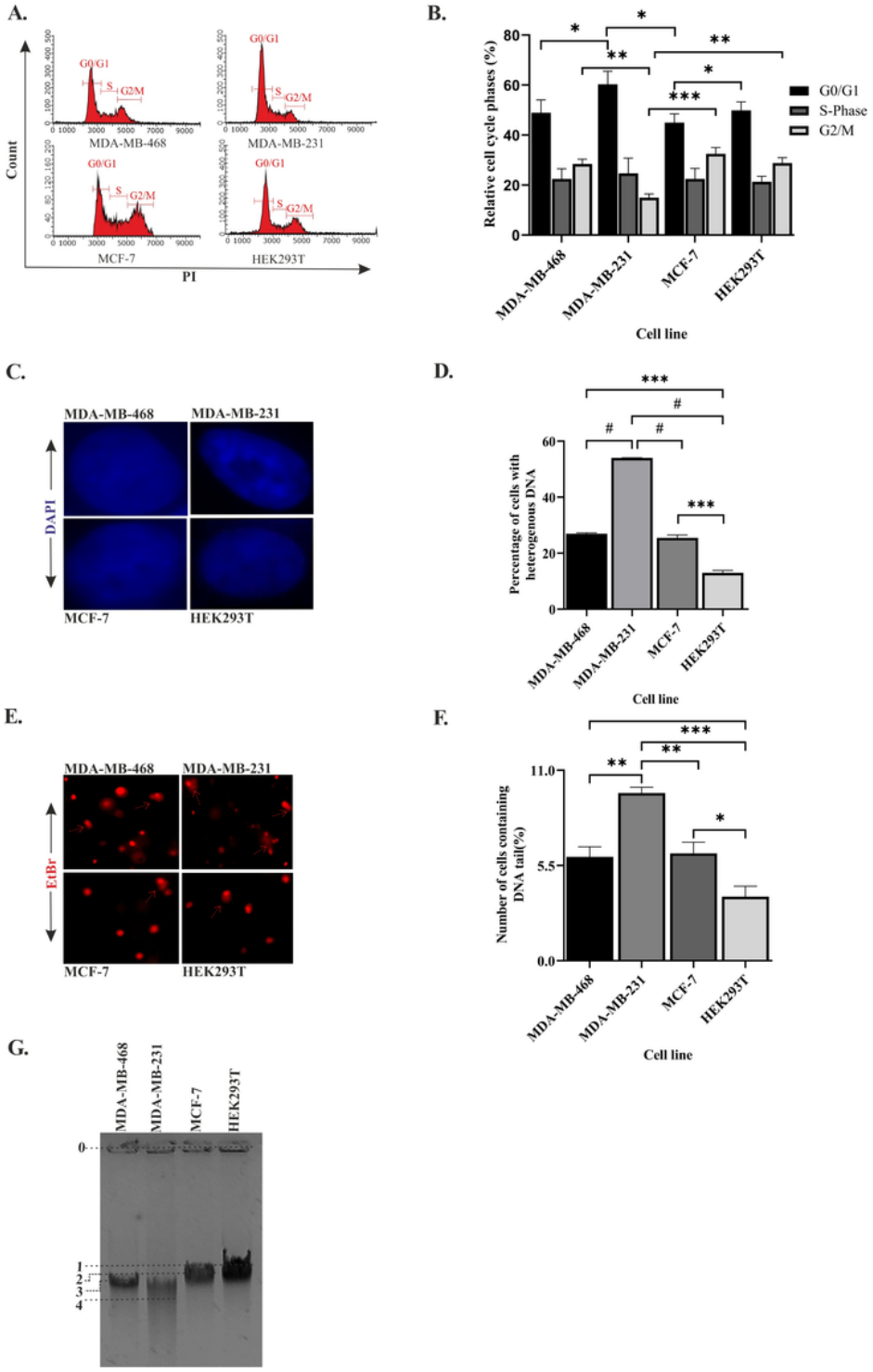

Figure 2.

Figure 2

The integrity of the genetic material differs between TNBC lines. A. MDAMB 231 cells have a significantly less G2/M population: Cell cycle analysis for different breast cancer cell lines, MDA-MB-468, MDA-MB-231, MCF-7 and normal cell line HEK293T, was performed in flow-cytometer. Histogram plot represents the distribution of 5000 cells into different phases of the cell cycle. B. Quantification of the cell population at different stages: Population of cells in different phases of the cell cycle were analysed and

plotted in a bar graph using In-cyte software of GUAVA Easycyte. C. Heterogeneous arrangement of the genetic material in MDAMB 231 cells suggest DNA damage: Representative cell images (100X magnification) of the above mentioned lines stained with DAPI shows the arrangement of the genetic material. D. Quantification of the increase in heterogeneity in the DNA of MDAMB 231 cells: Bar graph represents the qualitative analysis of around 200 cells with heterogeneous (blue patches) and homogeneous (evenly spread blue) DNA. E. Increase in tail formation in MDAMB 231 confirms more DNA damage: Representative image of cells having tails of fragmented DNA (comet) shows the extent of DNA damage in different cell types. The cells with the elongated tails are marked with broken red line arrows in the figure. F. Quantification of number of cells having tail DNA: The cells having comet (in all the fields captured) are plotted in the bar graph. A total of 150 cells were counted for each cell line. G. The fragmented DNA in MDAMB 231 cells moved the fastest through Agarose Gel electrophoresis: The figure represents the movement of DNA through Agarose gel ran at low voltage for longer time period. The migrated distance from the starting point 0, to the mid of the DNA band marked as 1, 2, 3 and 4 were measured. The distance traversed by HEK, MCF, MDA-MB 468 and MDA-MB 231 was 23.28 mm, 24.45 mm, 25.40 mm and 29.90 mm respectively. All the experiments were performed in biological triplicates. Data were analysed by one-way ANOVA. (SEM is shown as error bar. *P< 0.05, ** P < 0.005, *** P < 0.0005 and # P<0.0001)

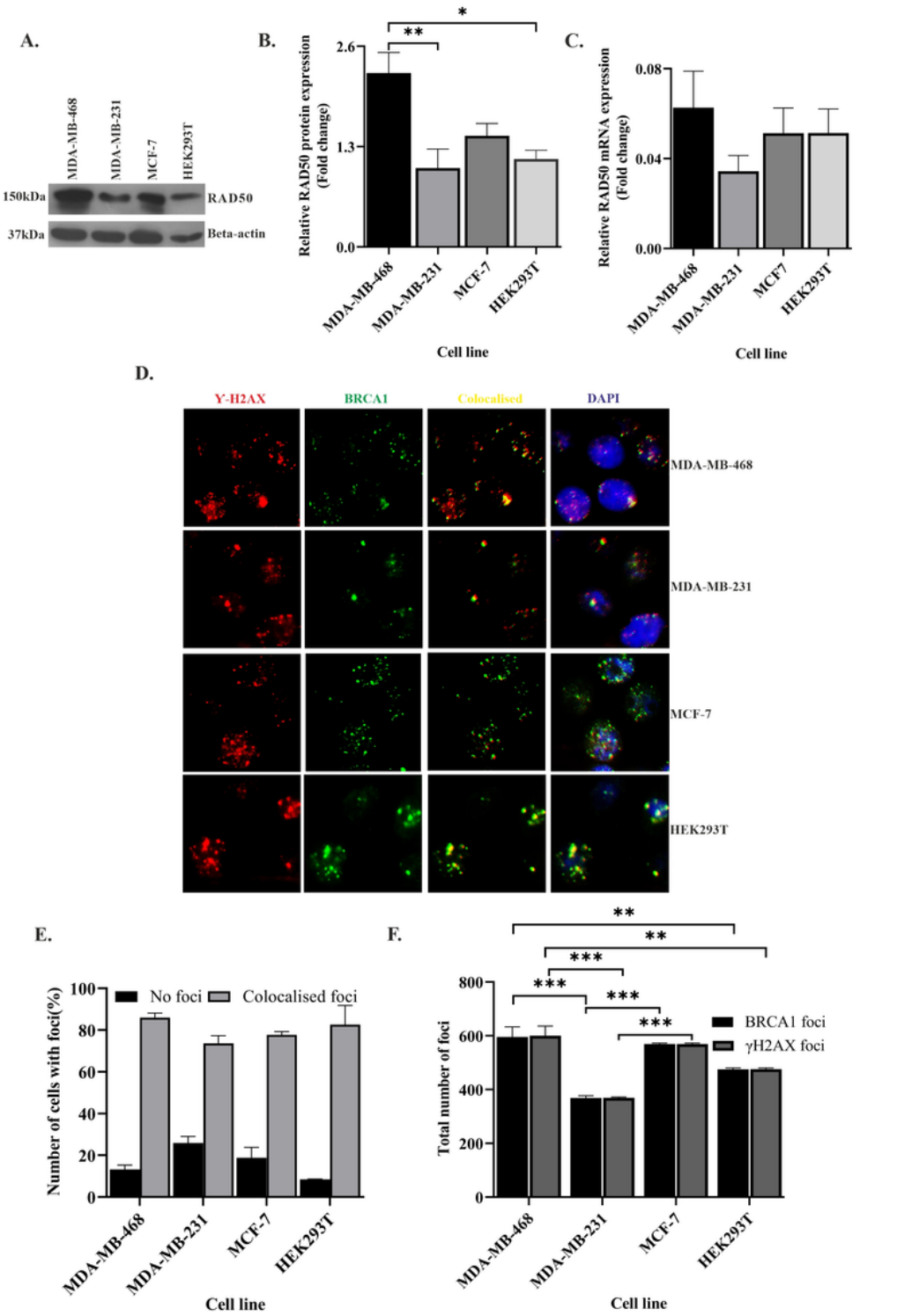

Figure 3.

Figure 3

DNA damage sensing abilities changes between different TNBC lines. A. Rad50 expression is compromised in MDAMB 231 cells: RAD50 expression was detected by western blot analysis of proteins extracted from TNBC cell lines MDA-MB-468 and MDA-MB-231, luminal type cell line MCF-7 and control line HEK293T using antibodies directed against Rad50 protein. ß-actin is considered as the loading control. B. Quantification of RAD50 protein expression in all the cell types: The intensity of the RAD50

bands from the Western analysis were quantified using Image J software. The values of band intensities were normalized with corresponding intensities of ß -actin. C. MDAMB 231 cells showed compromised expression of RAD50 transcript also: Expression studies were done with c-DNA (500 ng of RNA) from the above mentioned cell lines. The RAD50 expression was quantified by Real-time PCR from the technical triplicates and represented in the bar graph. ΔΔCt value was calculated from the Ct value of GAPDH and No template control (NTC). D. Formation of less H2AX foci in MDAMB 231: Representative fields of immunofluorescence assay showing gamma-H2AX and BRCA1 foci. The red dots in the first panel indicates the gamma-H2AX foci, Green dots in the second panel indicates the BRCA1 foci, yellow in the third panel indicated the co-localized foci and blue in the fourth panel shows the co-localization of H2AX-BRCA1 foci with the nucleus (DAPI) E. The colocalization of BRCA1 with H2AX is mildly compromised in MDAMB 231: The percentage of cells with no foci and co-localized foci were analysed by counting 200 cells and represented in the bar graph. F. H2AX- BRCA1 foci as the marker for DNA damage sensing is significantly compromised in MDAMB 231: The foci formation is analysed manually by scoring the red and green dots in 200 cells. MDA-MB 231 with less H2AX BRCA1 foci confirms the defect in damage sensing. All the experiments in this figure were performed in biological triplicates. Data were analysed by one-way and two-way ANOVA. (SEM is shown as error bar. *P< 0.05, ** P < 0.005 and *** P < 0.0005)

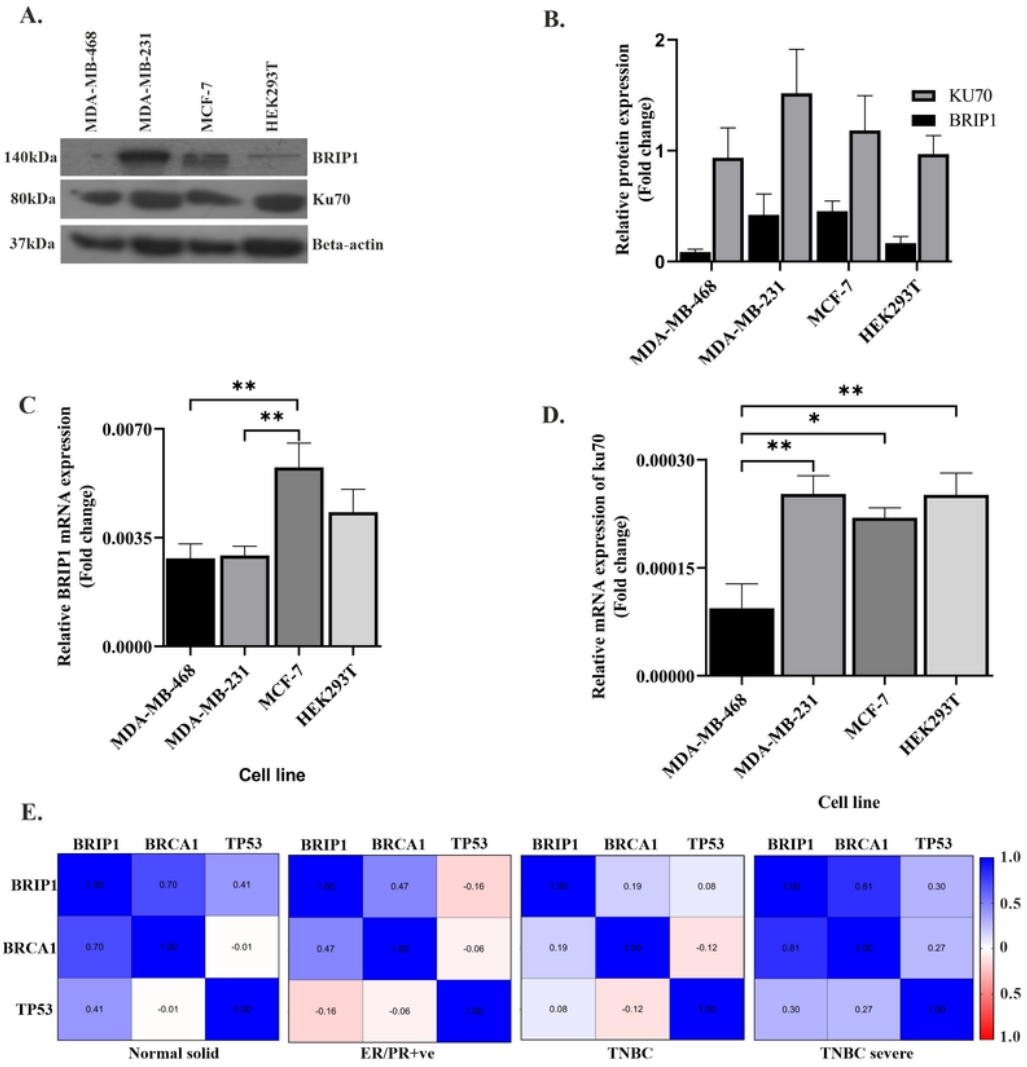

Figure 4.

Figure 4

Up regulation of the repair pathway due to accumulated damage: A. Over expressed HR and NHEJ proteins in MDA-MB-231 cells. HR marker BRIP1 and NHEJ marker KU70 was detected by western blot analysis of proteins extracted from TNBC cell line MDA-MB-468 and MDA-MB-231, luminal type cell line MCF-7 and control line HEK293T using corresponding antibodies. ß-actin is given as the loading control. B. Quantification of repair proteins in all the cell types. The intensity of the BRIP1 and KU70 bands from

the Western analysis were quantified using Image J software. The values of band intensities were normalized with corresponding intensities of ß - actin. C. The transcript level of BRIP1 is not functional in MDA-MB-231 cells: Expression studies were done with cDNA (500 ng of RNA) from the above lines. The bar graph represents the similar expression of BRIP1 in both the TNBC lines which was quantified by Real-time qPCR from the technical triplicates and represented in the bar graph. D. KU70 is over expressed in MDA-MB-231 cells compared to other TNBC lines. The functional analysis of KU70 was done with the extracted RNA from the above cell lines. The bar graph represents the expression of KU70 significantly more in case of MDAMB 231. The analysis was done with technical triplicates. $\Delta\Delta$Ct value was calculated from the Ct value of GAPDH, the housekeeping gene and no template control (NTC), the non-specific background. E. Association of BRCA1/ TP53 with BRIP1 shows up only in TNBC severe condition. Association between BRCA1, TP53 and BRIP1 in different tissues condition like the normal solid sample (N=119), ER/PR+ve (N=314), TNBC (N=95) and TNBC severe (N=9) is analysed by UCSC-Xena (TCGA) and represented in correlogram. Moving towards darker blue colour indicates an increase in positive correlation, whereas towards darker red indicates an increase in negative correlation. White colour indicates no correlation. All the experiments in this figure were performed in biological triplicates. Data were analysed by one-way ANOVA and Pearson correlation test. (SEM is shown as error bar. *P< 0.05 and ** P < 0.005)

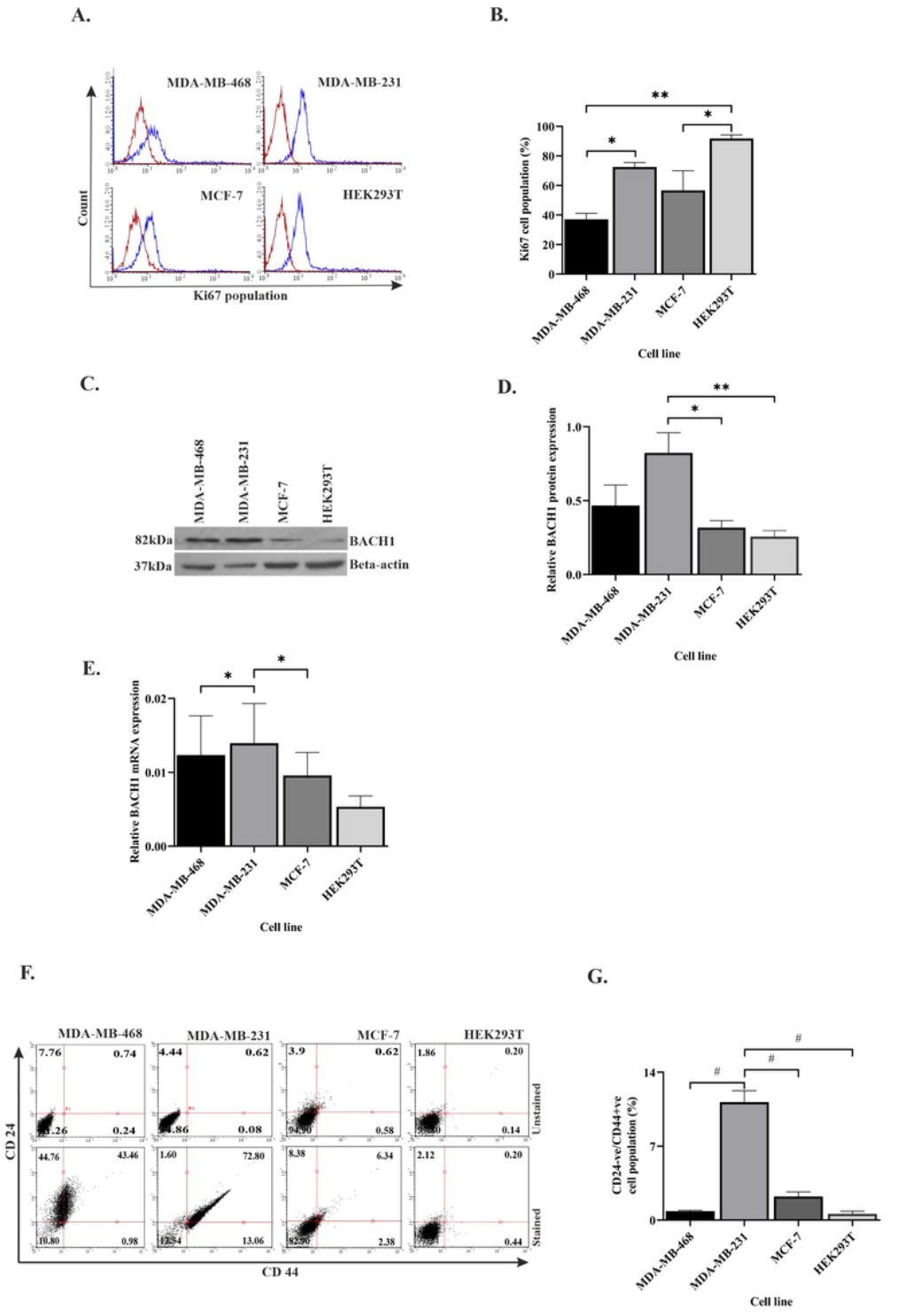

Figure 5.

Figure 5

Severity is highly dependent on repair pathways. A. ki67 is over expressed in MDA-MB-231 cells compared to other breast cancer subtypes. The proliferation of different TNBC cell lines MDA-MB-468 and MDA-MB-231, luminal type cell line MCF-7 and control line HEK293T were monitored by measuring the ki67 marker using Immunophenotyping assay and represented by histogram plots (Red line indicates the unstained population and the blue line indicates the ki67 stained population). B. Quantification of the

ki67 population in different cell types. The bar graph represents the percentages of cells having Ki67 expression which was measured by gating the ki67 population using GUAVA in-cyte software. C. The angiogenic/metastatic factor BACH1 over expresses in MDA-MB-231 cells. The protein expression of metastasis marker BACH1 was detected by western blot analysis of proteins extracted from the above mentioned cells, using the corresponding antibody. ß-actin is given as the loading control. D. Quantification of BACH1 protein using ImageJ software. The bar graph represents the intensity of BACH1 bands from Western analysis which was quantified using Image J software. The values of band intensities were normalized with corresponding intensities of ß - actin. E. MDAMB 231 cells showed over expression of BACH1 transcript also: Expression studies were done with c-DNA (500 ng of RNA) from the above mentioned cell lines. The BACH1 expression was quantified by RT- PCR from the technical triplicates and represented in the bar graph. $\Delta\Delta$Ct value was calculated from the Ct value of GAPDH and no template control (NTC). F. MDAMB 231 has more cancer stem cell population: The cancer stem cell population was analysed by Immunophenotyping assay. The dot plots represent the CD44+ve/CD24-ve stained (upper panel) and unstained (lower panel) population in different cell types. G. Quantification of the higher population of cancer stem cells in MDAMB 231: The bar graph represents the percentages of cells having CD44+ve/CD24-ve expression which was measured by gating the CD44+ve/CD24-ve population using GUAVA incyte software. All the experiments were performed in biological triplicates. Data were analysed by one-way ANOVA. (SEM is shown as error bar. *P< 0.05 and ** P < 0.005)

Supplementary Files

This is a list of supplementary files associated with this preprint. Click to download.

- Table1.pdf
- Table2.pdf
- Table3.pdf
- Feworiginalwesternblotssupplementary.pdf
- SupplementaryFinal.pdf